

## Research Article

# The Preventative Effect of Chitooligosaccharides against Chronic Alcoholic Liver Disease by Regulating Alcohol Metabolism, Fatty Acid Metabolism, and Intestinal Barrier Damage

Yuan Li,<sup>1</sup> Jiaqi Zou,<sup>1</sup> Hao Yin,<sup>2</sup> Mengyao Zhao <sup>1</sup>, and Liming Zhao <sup>1,2,3</sup>

<sup>1</sup>State Key Laboratory of Bioreactor Engineering,

R&D Center of Separation and Extraction Technology in Fermentation Industry, School of Biotechnology, East China University of Science and Technology, Shanghai 200237, China

<sup>2</sup>Organ Transplant Center, Shanghai Changzheng Hospital, Shanghai 200003, China

<sup>3</sup>Shanghai Frontiers Science Center of Optogenetic Techniques for Cell Metabolism, Shanghai 200237, China

Correspondence should be addressed to Mengyao Zhao; myzhao@ecust.edu.cn and Liming Zhao; zhaoliming@ecust.edu.cn

Received 27 July 2023; Revised 11 October 2023; Accepted 3 December 2023; Published 18 January 2024

Academic Editor: Jae Young Je

Copyright © 2024 Yuan Li et al. This is an open access article distributed under the Creative Commons Attribution License, which permits unrestricted use, distribution, and reproduction in any medium, provided the original work is properly cited.

Since chronic alcoholic liver disease (ALD) is a significant global health concern, several studies have shown that chitooligosaccharides (COS) exhibit hepatoprotective effects. This paper examined the COS protective effect on chronic ALD mice. Results showed that COS improved the lipid accumulation, liver injury, and oxidative stress levels in the mice while inhibiting cytochrome P450 protein 2E1 (CYP2E1) expression in the liver and promoting alcohol dehydrogenase (ADH) and acetaldehyde dehydrogenase (ALDH1) expression, indicating that COS could ameliorate alcohol metabolism. Moreover, COS intervention also enhanced the antioxidant capacity of the liver and upregulated peroxisome proliferator-activated receptor gamma coactivator 1 $\alpha$  (PGC-1), silent information regulator 1 (SIRT1), HO-1, and nuclear factor-erythroid 2-related factor 2 (NRF2) protein levels. In addition, COS increased peroxisome proliferator-activated receptor  $\alpha$  (PPAR $\alpha$ ), acyl-CoA oxidase (ACOX), acyl-CoA synthetase long-chain family member (ACSL), carnitine palmitoyltransferase 1A (CPT-1A), and carnitine palmitoyltransferase 2 (CPT2) protein levels by upregulating the fatty acid  $\beta$  oxidation pathway and restoring mitochondrial genesis. From a liver-gut axis perspective, COS enhanced intestinal barrier function by increasing the adhesion junction (AJ) and intestinal tight junction (TJ) protein expression. Therefore, COS displayed a protective ability against chronic ALD. The results provide a theoretical basis for utilizing supplemental dietary COS as a functional food alternative for treating chronic ALD.

## 1. Introduction

Among 200 million drinkers worldwide, more than 750 thousand are at risk of alcohol-related liver disease, placing significant economic strain on global healthcare systems [1]. An alcoholic fatty liver, hepatitis, and cirrhosis represent the main stages of chronic alcoholic liver disease (ALD) and can eventually evolve into liver cancer [2]. Fat accumulation represents the key stage for chronic ALD treatment [3]. Effectively preventing or delaying steatosis progression to more advanced chronic ALD stages has attracted significant attention [4, 5].

The pathogenesis of chronic ALD is highly complex and involves liver injury due to alcohol metabolic products,

oxidation-reduction system imbalance [6], fat accumulation caused by abnormal fat metabolism [7], intestinal barrier damage, and intestinal microecological disturbance [8]. The main metabolic alcohol pathways in the body are alcohol dehydrogenase (ADH)/acetaldehyde dehydrogenase (ALDH) and the microsomal ethanol oxidation system [9]. High alcohol intake shifts the alcohol metabolism from ADH to cytochrome P450 protein 2E1 (CYP2E1) metabolism [10]. Long-term alcohol consumption activates CYP2E1 in the liver, changing it into the main alcohol-metabolizing enzyme, which accelerates the conversion of alcohol into acetaldehydes, producing substantial reactive oxygen species (ROS) levels [10]. ROS accumulation further

promotes oxidative stress and mitochondrial function damage, ultimately hindering fatty acid  $\beta$  oxidation [11]. Therefore, impaired fatty acid  $\beta$  oxidation in the mitochondria is considered the leading cause of alcohol-related fat accumulation [7, 12]. Moreover, recent studies have shown the importance of the enterohepatic axis in chronic ALD pathogenesis. ALD patients typically exhibit disturbed intestinal microecologies and damaged intestinal barriers [13]. Intestinal adhesion junction (AJ) and tight junction (TJ) protein degradation increases intestinal permeability, allowing endotoxins, such as LPS and harmful bacteria to reach the liver via enterohepatic circulation. LPS targets Kupffer cells and hepatocytes in the liver, inducing the release of inflammatory factors and chemokines from the cells, causing a secondary hit to the liver and aggravating chronic ALD [14, 15].

The corticosteroids, hexadione, theobromine, and other drugs used for treating chronic ALD are limited by their side effects [16]. Although abstinence from alcohol is currently the most effective and least toxic clinical procedure against chronic ALD, sudden alcohol consumption termination may aggravate the symptoms [17]. Therefore, the availability of safe, effective, and diverse therapeutic agents is crucial for treating and preventing chronic ALD. Chito oligosaccharides (COS) have attracted widespread attention due to their excellent liver protective properties. COS displays no toxic side effects on the liver and does not interfere with the lipid metabolism of normal rats [18]. Moreover, COS can counteract acetaminophen-induced liver injury and  $\text{CCl}_4$ -induced liver fibrosis and damage [19–21] while improving nonalcoholic fatty liver disorder and relieving lipid accumulation and inflammation [22, 23]. Luo et al. showed that COS protects L02 cells from acute alcohol exposure by activating nuclear factor-erythroid 2-related factor 2 (NRF2) and inhibiting the apoptotic pathway, suggesting that COS may protect against alcoholic injury [24]. Moreover, Park et al. indicated that COS can activate ADH and ALDH, promote alcohol metabolism, and ameliorate acute liver toxicity due to alcohol exposure [25]. However, the mechanism behind the protective effect of COS against ALD, especially chronic ALD, remains unclear.

Therefore, this paper examined the potential protective impact of different COS doses on chronic alcoholic liver injury in mice, focusing on the changes in alcohol metabolism, lipid metabolism, and liver-gut axis. The results will provide a theoretical basis for utilizing supplemental dietary COS as a functional food alternative for treating chronic ALD.

## 2. Materials and Methods

**2.1. Animals and Experimental Methods.** COS were prepared in our laboratory. The chitosan mixtures were purified by ultrafiltration and nanofiltration, separated using cation exchange resins, and desalted and freeze-dried and finally high purity COS is obtained [26]. The identification of COS was investigated using electrospray ionization source mass, and high-performance liquid chromatography (HPLC) results are shown in Supplementary Figures 1 and 2. Shanghai

JieSijie Laboratory Animal Co. Ltd. supplied the six-week-old male C57BL/6J mice. Approval for the experiments was provided by the Ethics Committee of East China University of Science and Technology (certificate no. ECUST-2022-082), which was conducted according to the China Institutional Animal Care and Use Committee requirements. The animal room was maintained at a temperature of  $23.0 \pm 1.0^\circ\text{C}$ , a relative humidity of 40–70%, artificially illuminated with a 12 h light/dark cycle, and air exchanges of 15 times/h.

After a one-week adaptation phase, the mice were divided into six random groups ( $n=10$ ): (1) normal control group (Con), (2) alcoholic liver model group (Mod), (3) silymarin group (Sily,  $63 \text{ mg}\cdot\text{kg}^{-1}\cdot\text{day}^{-1}$  silymarin), (4) low-dose COS group (COS-L,  $125 \text{ mg}\cdot\text{kg}^{-1}\cdot\text{day}^{-1}$  COS), (5) medium-dose COS group (COS-M,  $250 \text{ mg}\cdot\text{kg}^{-1}\cdot\text{day}^{-1}$  COS), and (6) high-dose COS group (COS-H,  $500 \text{ mg}\cdot\text{kg}^{-1}\cdot\text{day}^{-1}$  COS). The Mod group received an alcohol-adapted diet for 6 d, followed by ad libitum feeding for eight weeks with either the Lieber–DeCarli control or the ethanol-containing Lieber–DeCarli diet (5% ethanol w/v) [27] (Figure 1). Body weight was monitored once weekly. The mice fasted for 12 h before euthanasia, after which blood and tissue samples were collected. The serum and liver tissue were kept at  $-80^\circ\text{C}$  storage until analysis.

**2.2. Biochemical Test.** The mouse plasma was left to stand for 3 h at room temperature and centrifuged for 15 min at  $625 g$ , after which the serum was collected. Tissue homogenates were prepared using the same part of the liver at a tissue weight ratio of saline = 1 : 9. A commercial kit (Jiancheng Biotech, China) was used to determine the ALDH, ADH, glutathione (GSH-PX), malondialdehyde (MDA), lactate dehydrogenase (LDH), alkaline phosphatase (ALP), aspartate aminotransferase (AST), alanine aminotransferase (ALT), high-density lipoprotein (HDL-C), low-density lipoprotein (LDL-C), total cholesterol (TC), and triglyceride (TG) levels in serum and tissues. All experimental procedures were performed according to the standards and protocols of the manufacturers.

**2.3. Histological Analysis.** The liver and ileum tissues of the mice were fixed with 10% formalin, embedded in paraffin, sliced into  $5 \mu\text{m}$  sections, and stained with hematoxylin-eosin (HE). The stained sections were examined using a microscope and subjected to pathological analysis. Frozen mouse liver tissue sections were fixed in a 4% neutral paraformaldehyde solution and subjected to Oil Red O (ORO) staining, after which the samples were examined and photographed using a microscope.

**2.4. Immunofluorescence Staining.** ROS production was determined using the DHE cell-permeable fluorophore. ROS oxidized the DHE dye to a different product that emitted red fluorescence by binding to chromosomal DNA, ultimately revealing ROS in the cells. DAPI was used to label the cells by crossing the cellular module and binding to DNA strands to

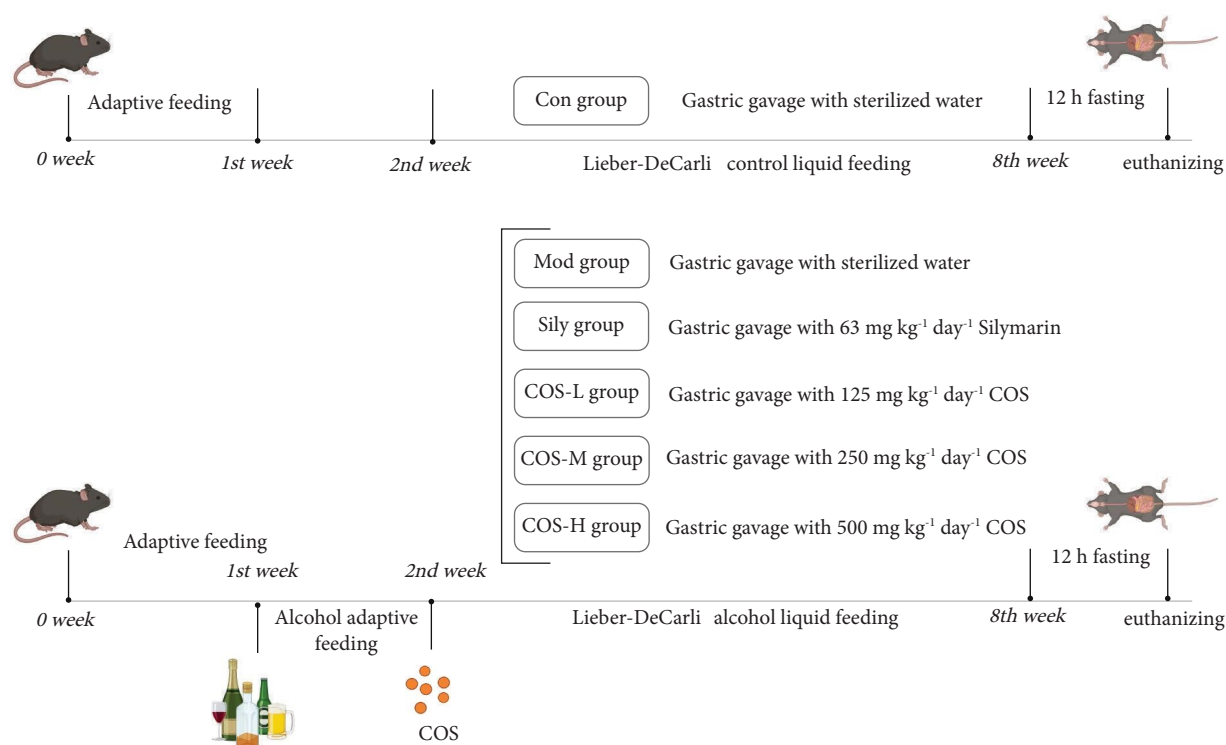


FIGURE 1: Animal grouping diagram.

emit a blue fluorescence. Frozen liver sections were incubated with a  $10\ \mu\text{M}$  DHE probe for 20 min in the dark, and DAPI was added for nuclear staining, after which the samples were examined and photographed using a fluorescence microscope.

**2.5. The Protein Expression Determination via Western Blot Analysis.** The proteins were extracted from the animal tissues using RIPA lysate and centrifuged for 10 min at  $10000\ g$  and  $4^\circ\text{C}$ , after which the supernatant was collected. Then, a BCA kit was used to determine the protein concentration.

For western blotting, the proteins separated via SDS-PAGE were placed on PVDF membranes, which were sealed using 5% skim milk powder and washed with TBST. The membranes were subjected to overnight incubation at  $4^\circ\text{C}$  with specific primary antibodies. GAPDH (10494-1-AP), acyl-CoA oxidase (ACOX) (10957-1-AP), carnitine palmitoyltransferase 1A (CPT1A) (15184-1-AP), and carnitine palmitoyltransferase 2 (CPT2) (26555-1-AP) were obtained from Proteintech (Wuhan, China), while  $\beta$ -actin (4970) was supplied by Cell Signaling Technology (Danvers, MA, USA). CYP2E1 (A2160), silent information regulator 1 (SIRT1) (A11267), peroxisome proliferator-activated receptor gamma coactivator 1 $\alpha$  (PGC-1) (A12348), peroxisome proliferator-activated receptor  $\alpha$  (PPAR $\alpha$ ) (A3123), and acyl-CoA synthetase long-chain family member (ACSL) (A227379) were acquired from ABclonal (Wuhan, China), while Wanleibio (Shenyang, China) provided NRF2 (WL02135), HO-1 (WL02400), ALDH (WL02762), claudin3 (WL00910),  $\beta$ -catenin (WL 0962a), and E-cadherin (WL01482). ADH was

supplied by Santa Cruz Biotechnology (Texas, USA), while zonula occluden-1 (ZO-1) (TA5145), occludin (T55997), and claudin4 (TA5350) were obtained from ABmart (Shanghai, China). The samples were washed with TBST and incubated at room temperature with HRP-labelled secondary antibodies solution for 1 h. The blots were determined using an ECL luminescent solution (Biosharp, China) detection substrate in a Tanon 4200 imaging system. The protein band signals were quantified via ImageJ software.

**2.6. Molecular Docking Simulation.** AutoDock Vina was used for the molecular docking of COS to CYP2E1 and PPAR $\alpha$ . CYP2E1 (PDB ID: 3lc4) and PPAR $\alpha$  (PDB ID: 6kxx) were retrieved from the RCSB Protein Data Bank (<https://www.rcsb.org/>). Before virtual docking, the protein structure was used to remove ligand, water, hydrogenation, charge, and other operations, and the file was saved as a ".pdb" file. The ligand-protein interactions were assessed according to the predicted binding energies (kcal/mol), while the PyMOL software and the Proteins Plus website (<https://proteins.plus/>) were used to demonstrate hydrogen bond, hydrophobic group and charged group formation, and bonding.

**2.7. Data Analysis.** GraphPad Prism version 8.0 was used for statistical data analysis, while one-way analysis of variance (ANOVA) was employed for multiple group comparisons. The data were presented as the mean  $\pm$  standard deviation (SD). Different uppercase letters denoted the significant differences between the groups ( $P < 0.05$ ), while the same uppercase letters signified no significant differences between the groups ( $P > 0.05$ ).

### 3. Results

**3.1. The Effect of COS on the Growth of Chronic ALD Mice.** Figures 2(a) and 2(b) show the body weight changes in the mice during the experiments. After eight weeks, the body weight growth rates of the alcohol-fed mice were significantly lower ( $P < 0.05$ ) than those of the Con group. The liver index of the Mod group substantially exceeded the Con group, suggesting that long-term alcohol exposure led to liver damage (Figure 2(c),  $P < 0.05$ ). COS intervention increased the body weight growth rate and decreased the liver index. Significant differences were evident between the COS-H and Mod groups (Figure 2(c),  $P < 0.05$ ), indicating that COS intake attenuated the negative impact of alcohol on the growth and development of mice and improved alcoholic liver damage.

**3.2. The Effect of COS on the Liver Injury, Lipid Levels, and Oxidative Stress of Chronic ALD Mice.** The biochemical indicators related to liver damage, lipid profiles, and oxidative stress in the serum and liver were measured to assess the effect of COS intervention on chronic ALD. The AST, ALT, ALP, and LDH levels in the Mod group were considerably higher than in the Con group ( $P < 0.05$ ), decreasing dose-dependently after low-, medium-, and high-dose COS intervention (Figure 3(a)). The high-dose COS group ( $P < 0.05$ ) displayed the most significant effect, returning to the Con group level, suggesting that COS intervention alleviated the liver injury caused by long-term alcohol exposure.

The TG, TC, and LDL-C levels increased significantly in the serum and livers of the mice after ethanol exposure, while the HDL-C levels displayed a considerable decline (Figures 3(b) and 3(c),  $P < 0.05$ ). Compared with the Mod group, COS reduced LDL-C, TG, and TC levels, as well as serum and liver lipid profiles, while increasing HDL-C levels. This indicated that COS intervention effectively reduced the liver and serum lipid levels in the mice and alleviated the abnormal lipid profiles caused by long-term alcohol exposure.

Since oxidative stress is a recognized pathology of an alcoholic liver [24], the effect of COS was examined further. As shown in Figure 3(d), the GSH-PX, SOD, and CAT levels were significantly higher ( $P < 0.05$ ) in the livers of the COS group than in the Mod group, while the MDA content was notably lower ( $P < 0.05$ ). This suggested that COS improved the antioxidant capacity of the mice while reducing oxidative alcoholic liver damage.

The pathological changes in the liver of each group were examined to further verify the effect of COS intervention. As illustrated in Figure 3(e), HE staining showed that the hepatocytes of the Mod group mice displayed considerable liver damage and fat vacuolation (black arrow). Although COS treatment improved the severe alcohol-induced liver damage and reduced the degree of fat vacuolation, the effect was similar to that of silymarin. The most significant protective effect was observed in the COS-H group, which almost returned to normal levels (Figure 3(e)). In addition, after ORO staining, the Mod group exhibited numerous red areas compared with the Con group, indicating severe alcohol-induced hepatic steatosis, while different COS doses effectively alleviated hepatic fat accumulation (Figure 3(f)).

**3.3. The Effect of COS on the Alcohol Metabolism of the Chronic ALD Mice.** The CYP2E1, ADH, and ALDH enzymes are vital for alcohol metabolism in the liver [28]. Their activity and protein levels were measured in the livers of the chronic ALD mice to determine whether COS affected alcohol metabolism.

As illustrated in Figures 4(a) and 4(b), the ADH in the Mod group was significantly inhibited ( $P < 0.05$ ) compared with the Con group, while COS intervention substantially increased the ADH and ALDH activities ( $P < 0.05$ ). Furthermore, although alcohol significantly inhibited ADH and ALDH ( $P < 0.05$ ), the CYP2E1 expression increased considerably ( $P < 0.05$ ). COS dose-dependently reversed this trend (Figures 4(c) and 4(d)). Moreover, COS produced hydrogen bonds with CYP2E1 Thr303 and yielded a docking score of  $-6.0$  kcal/mol (Figure 4(e)), indicating that it inhibited CYP2E1 activity. Martikainen et al. showed that active CYP2E1 inhibition mainly occurred via electrostatic interaction with Thr303 amino acids [29]. Therefore, the results suggested that COS inhibited CYP2E1 and activated ADH and ALDH, contributing to alcohol metabolism in chronic ALD.

**3.4. The Effect of COS on Oxidative Stress and Mitochondrial Damage in the Chronic ALD Mice.** The potential anti-oxidative mechanism of COS was explored further. Considerable ROS accumulation was evident in the livers of the Mod group mice (Figure 5(a)), while the NRF2 and HO-1 expression was substantially downregulated after long-term alcohol exposure (Figures 5(b) and 5(c),  $P < 0.05$ ). Different COS doses significantly upregulated the NRF2 and HO-1 expression (Figures 5(b) and 5(c),  $P < 0.05$ ), promoting the antioxidant capacity of the body. This was consistent with the results showing that COS increased GSH-PX, CAT, and SOD antioxidant enzyme activity in the liver tissues.

ROS mainly attacks and damages mitochondria. To examine the effect of COS on the mitochondria of chronic ALD mice, the mitochondrial state in the liver was observed. Liver electron microscopy showed abnormal structural mitochondrial swelling in the Mod group (Figure 5(d)). SIRT1 is located upstream of peroxisome proliferator activator receptor  $\gamma$  coactivator 1 $\alpha$  (PGC-1 $\alpha$ ), representing essential nuclear proteins during mitochondrial biogenesis and energy regulation. The Mod group displayed lower SIRT1 and PGC-1 $\alpha$  expression than the Con group, while COS consumption significantly enhanced these levels (Figures 5(e) and 5(f),  $P < 0.05$ ), indicating that COS promoted mitochondrial synthesis regulation and function restoration.

**3.5. The Effect of COS on the Fatty Acid  $\beta$  Oxidation in the Chronic ALD Mice.** SIRT1 and PGC-1 are thought to be closely related to fatty acid oxidation [5], while fat accumulation caused by alcohol is associated with the down-regulation of fat  $\beta$  oxidation. The fatty acid  $\beta$  oxidation-related protein expression in the liver was measured. Consistent with previous reports, proteins associated with fat oxidation were inhibited in the livers of the Mod group,

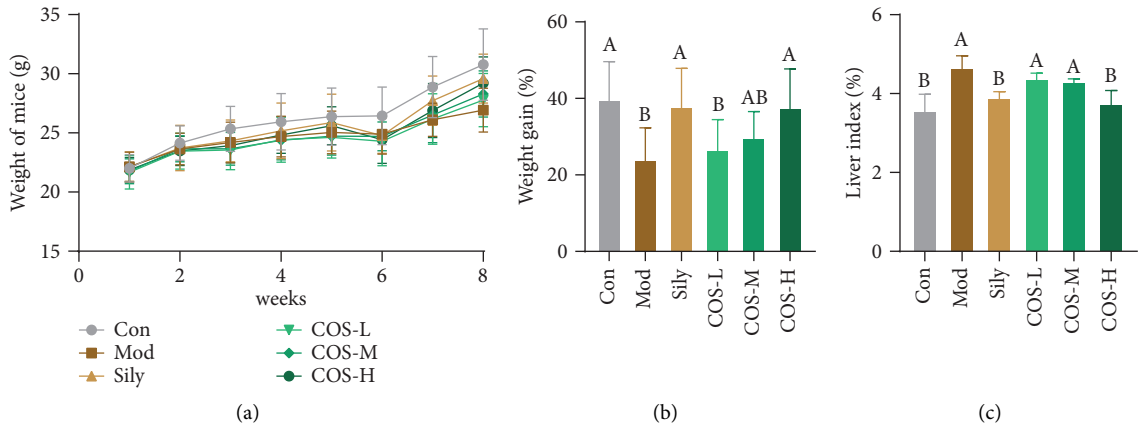


FIGURE 2: The effect of COS on the growth of mice. The (a) body weight, (b) weight gain, and (c) liver index changes in the mice. Data are shown as the mean  $\pm$  SD ( $n = 10$ ). Significant differences between the groups ( $P < 0.05$ ) are denoted by individual uppercase letters.

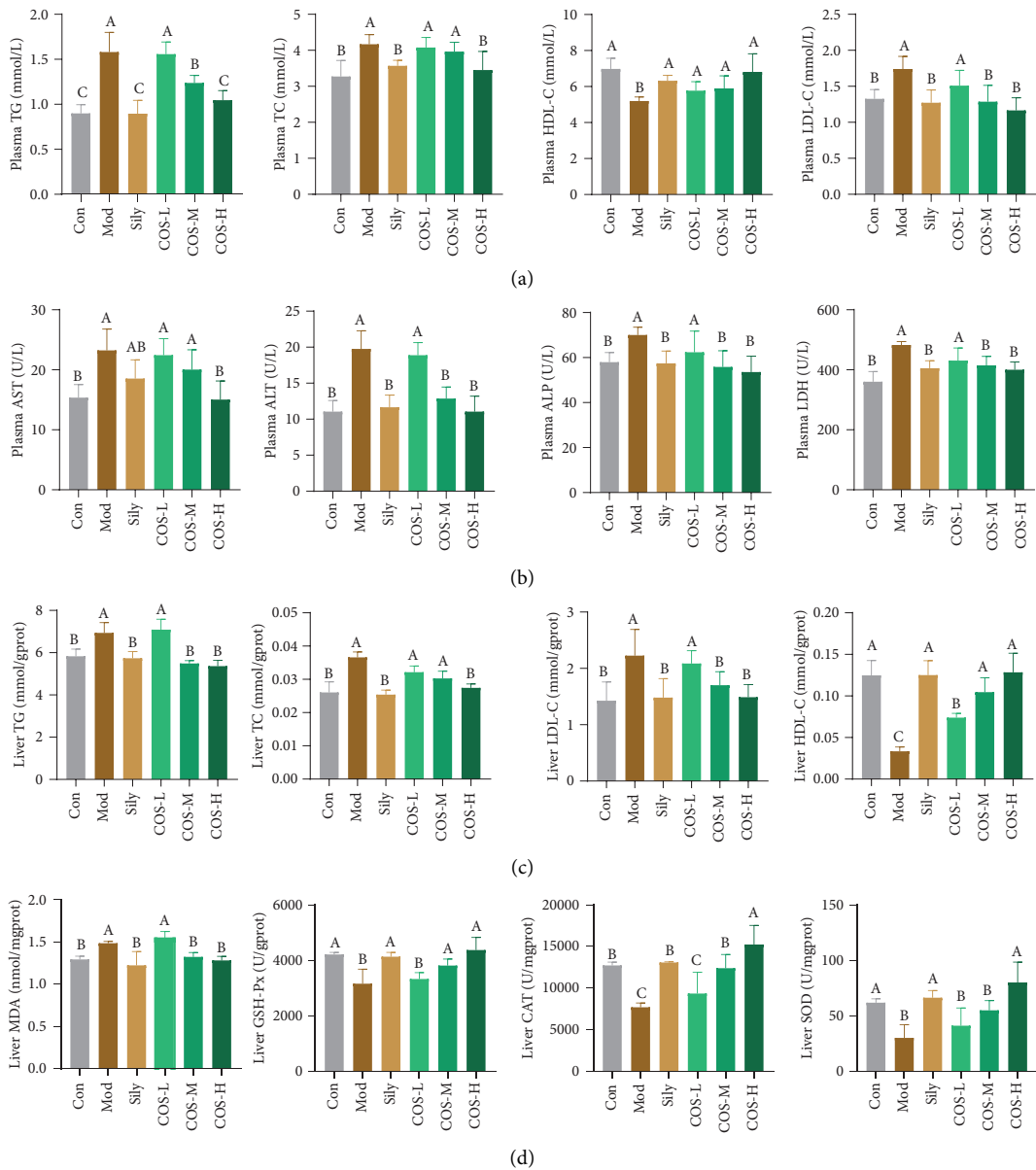


FIGURE 3: Continued.



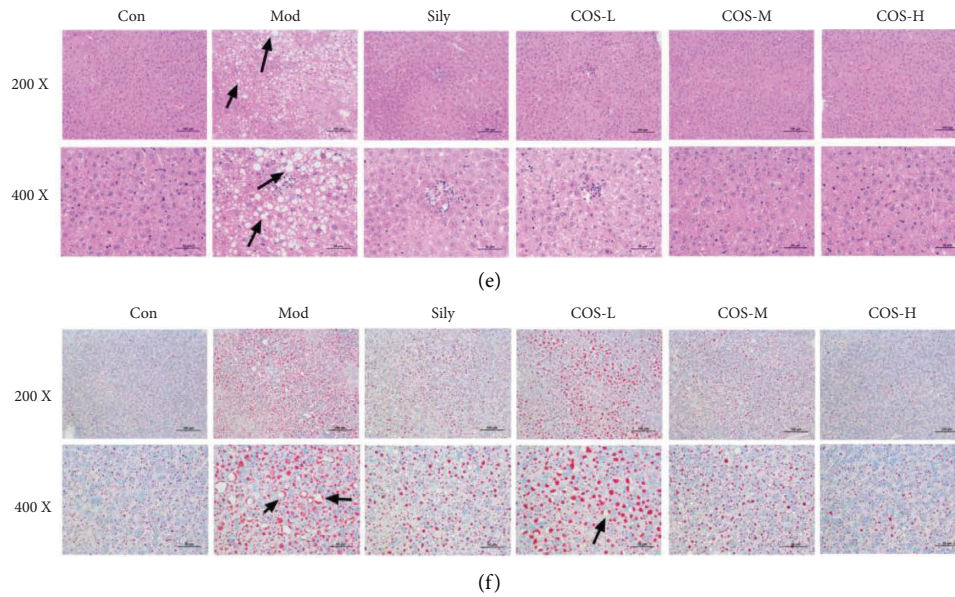


FIGURE 3: COS improves the serum and liver biochemical indexes of the chronic ALD mice. (a) The serum AST, ALT, ALP, and LDH levels. (b) The serum HDL-C, LDL-C, TC, and TG levels. (c) The liver HDL-C, LDL-C, TC, and TG levels. (d) The liver SOD, CAT, and GSH-PX activities and MDA levels. The black arrows indicate macrovesicular steatosis and lipid droplet accumulation. (e) Liver tissue HE staining at 200 × (scale bar = 100 μm) and 400x magnification (scale bar = 50 μm). (f) Liver tissue ORO staining at 200 × (scale bar = 100 μm) and 400x magnification (scale bar = 50 μm). The black arrows indicate macrovesicular steatosis and lipid droplet accumulation. Data are shown as the mean ± SD ( $n \geq 3$ ). Significant differences between the groups ( $P < 0.05$ ) are denoted by individual uppercase letters.

while COS consumption activated fat metabolism-related proteins, including PPAR $\alpha$ , ACOX, ACSL, CPT1A, and CPT2 (Figures 6(a) and 6(b),  $P < 0.05$ ). Although chronic alcohol exposure inhibited fatty acid oxidation in the liver, COS normalized fat metabolism and accelerated hepatic fat elimination.

Since PPAR $\alpha$  regulated fatty acid  $\beta$  oxidation, this study selected PPAR $\alpha$  and COS for molecular docking to investigate their conformational relationships. The results are shown in Figure 6(c), presenting a chitosan with a PPAR $\alpha$  docking score of  $-5.2$  kcal/mol. Moreover, COS formed six hydrogen bonds in the active PPAR $\alpha$  site, particularly with Tyr464, His440, Tyr314, and Ser280, representing the four key amino acids for existing PPAR $\alpha$ -agonists [30], suggesting that COS effectively played a significant role in the active PPAR $\alpha$  pocket.

The free fatty acids (FFA) content in the liver was measured and presented as a heat map (Figure 6(d)). Chronic alcohol consumption increased the arachidonic,  $\alpha$  linoleic, heptadecanoic, linoleic, and caprylic acid levels in the liver while decreasing the myristic acid and myristoleic content. However, these fatty acids returned to normal levels after COS intervention, indicating enhanced fatty acid  $\beta$  oxidation in the mouse livers.

**3.6. The Effect of COS on the Intestinal Barrier Function of the Chronic ALD Mice.** The ilea of the mice were histologically analyzed to determine whether COS contributed to intestinal barrier restoration. HE staining indicated intestinal villi shortening and deformation in the mice chronically exposed to alcohol, while COS reduced the alcohol damage

to the intestinal tract (Figure 7(a)). The AJ/TJ protein expression in the intestinal tract is closely related to the integrity of the intestinal barrier. Although the AJ (E-cadherin and  $\beta$ -catenin) and TJ (including ZO-1, claudin4, claudin3, and occludin) protein expression levels decreased significantly in the intestinal tracts of the Mod group, they increased considerably after dose-dependent COS intervention (Figures 7(b)–7(e),  $P < 0.05$ ), indicating that COS effectively improved intestinal permeability and protected intestinal barrier function.

#### 4. Discussion

Although chronic ALD increases the economic burden on society, effective clinical treatment is lacking [16, 17, 31, 32]. Several pilot studies have suggested the potential beneficial impact of COS on severe alcoholic liver damage. However, the potential mechanism behind the effect of COS on chronic ALD remains mostly unclear. This study used COS intervention in C57BL/6J mice receiving a Lieber–DeCarli diet for eight weeks to assess its protective impact on chronic ALD. The results indicated that COS restored the pathological chronic ALD process by improving alcohol metabolism and alleviating oxidative stress, mitochondrial damage, fat accumulation in the liver, and intestinal barrier integrity (Figure 8).

COS displayed a significant protective effect against liver injury, lipid disorders, and oxidative damage in mice chronically exposed to alcohol. COS intervention substantially reduced the LDH, ALP, ALT, and AST activities in the serum of the mice and mitigated liver damage resulting

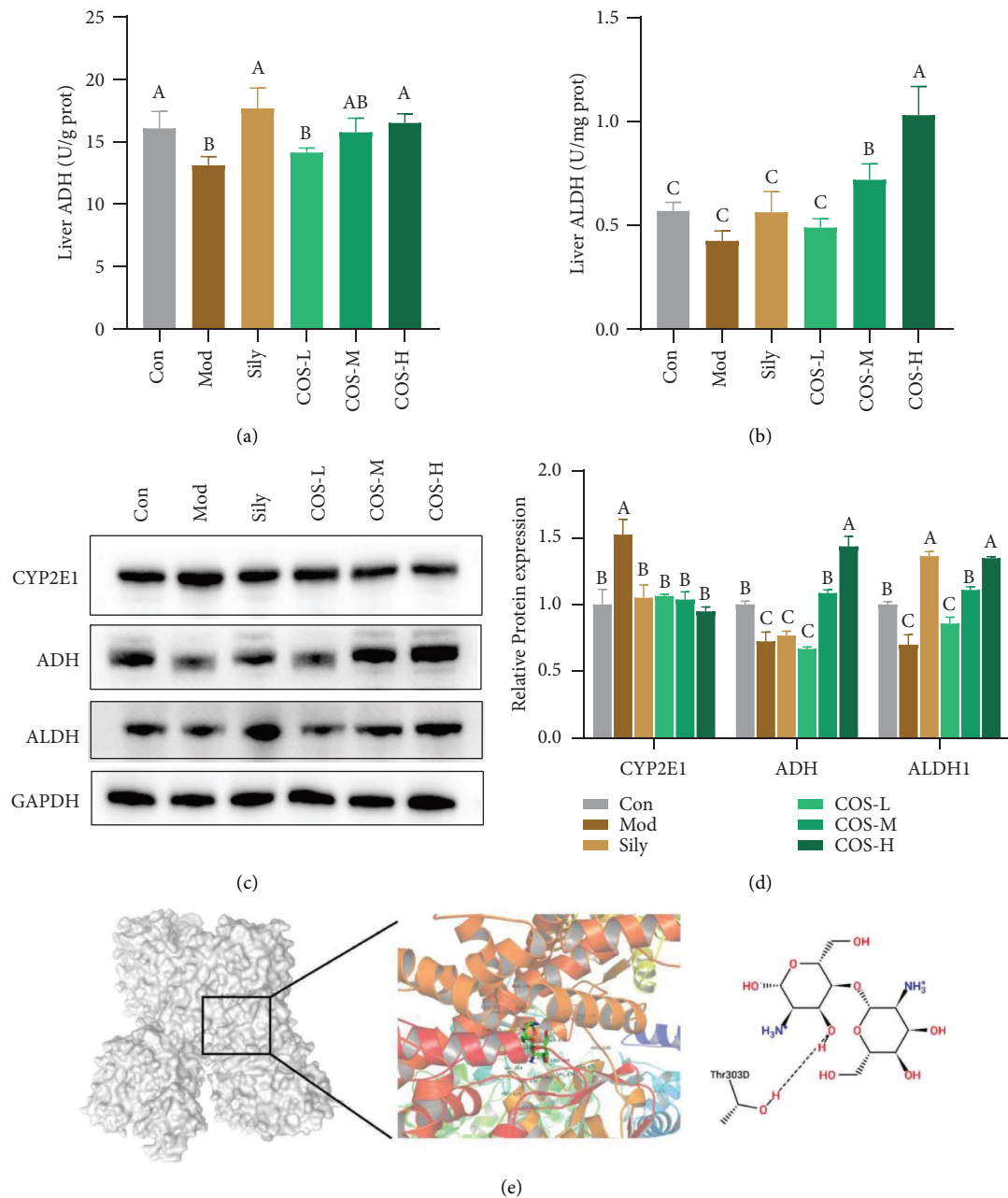


FIGURE 4: COS improves hepatic alcohol metabolism in chronic ALD mice. The liver (a) ADH and (b) ALDH activities. (c) The western blot image. (d) The relative protein expression analysis of CYP2E1, ADH, and ALDH is normalized to GAPDH. (e) The binding patterns, key interactions, and corresponding 2D maps of the active COS sites (green) relative to CYP2E1, as revealed by molecular docking. Data are shown as the mean  $\pm$  SD ( $n \geq 3$ ). Significant differences between the groups ( $P < 0.05$ ) are denoted by individual uppercase letters.

from long-term alcohol exposure. Furthermore, the LDL-C, TC, and TG levels in the serum and liver were reduced, while the HDL-C content, abnormal lipid levels, and liver fat accumulation caused by alcohol were improved. In addition, COS reduced the MDA content in the liver and increased the CAT, GSH-PX, and SOD activities, improving the antioxidant capacity of the body and reducing alcohol-induced oxidative stress.

The development of chronic ALD is associated with changes in the metabolism of alcohol in the body. When alcohol is metabolized by CYP2E1, a large amount of ROS is

produced, causing oxidative damage [33]. COS intervention inhibited CYP2E1 and downregulated protein expression, improving the metabolic alcoholic pathway. Furthermore, COS activated the NRF2/HO-1 pathway, upregulated downstream antioxidant enzymatic activity, enhanced antioxidative capacity, and reduced oxidative stress. In addition, COS activated NRF2 during acute pancreatitis [34] and acetaminophen-induced liver injury [20] to alleviate oxidative stress.

Increased oxidative stress promotes oxidative mitochondrial phosphorylation, destroying the mitochondrial membrane potential and leading to damage [35]. PGC-1

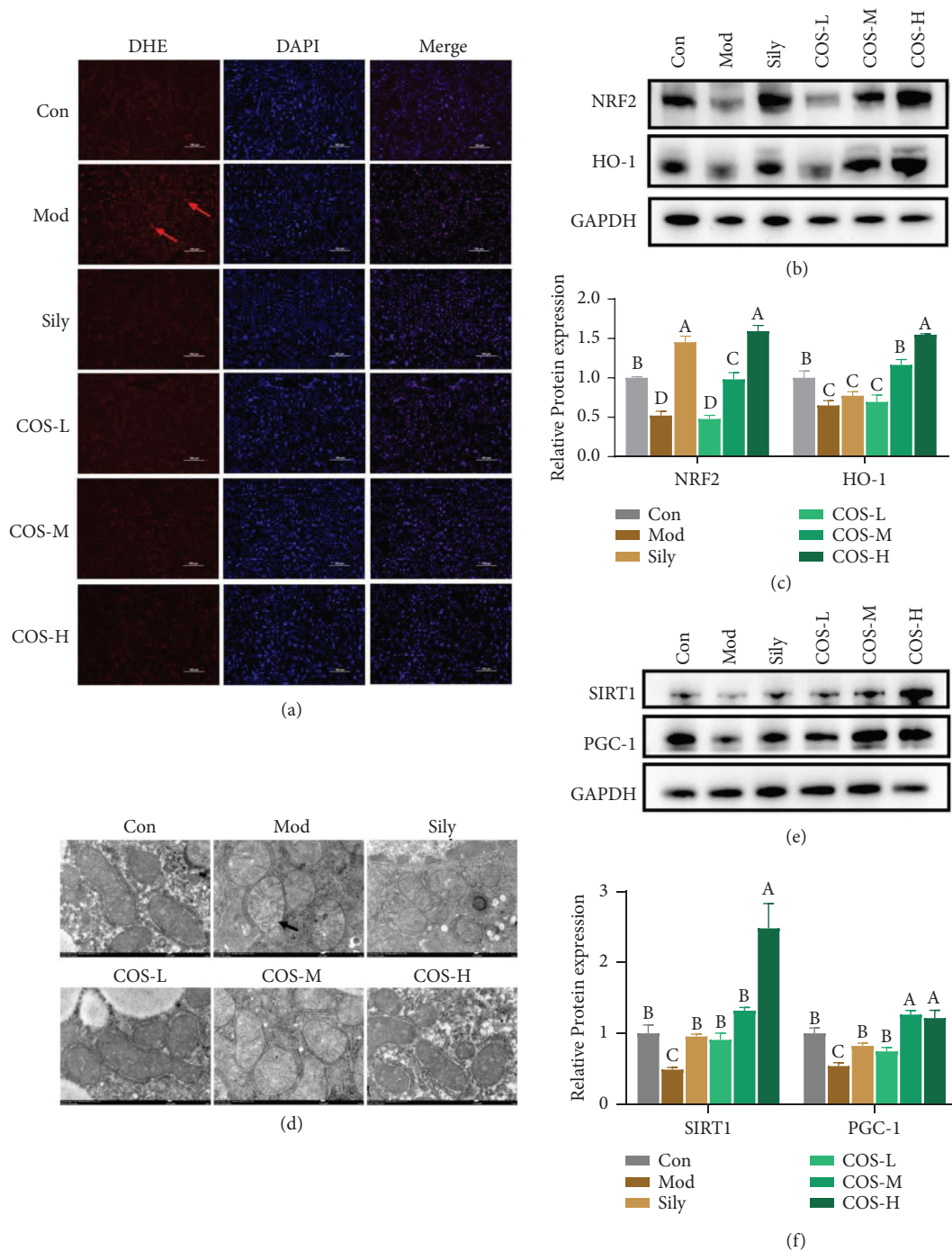


FIGURE 5: COS inhibits hepatic oxidative stress and mitochondrial damage in the chronic ALD mice. (a) The DHE staining of liver sections (scale bar = 100  $\mu\text{m}$ ). The red arrows indicate ROS accumulation. (b) The western blot image of NRF2 and HO-1. (c) The relative NRF2 and HO-1 protein expression is normalized to GAPDH. (d) The representative TEM images of the liver tissue (scale bar = 1.0  $\mu\text{m}$ ). The black arrows indicate swollen and damaged mitochondrial accumulation. (e) The western blot image of SIRT1 and PGC-1. (f) The relative SIRT1 and PGC-1 protein expressions are normalized to GAPDH. Data are shown as the mean  $\pm$  SD ( $n \geq 3$ ). Significant differences between the groups ( $P < 0.05$ ) are denoted by individual uppercase letters.

controls mitochondrial biogenesis, while SIRT1 represents the upstream PGC-1 factor, acting as a metabolic and redox sensor of energy state changes in the body [36]. COS promotes the SIRT1 and PGC-1 translation levels in chronic ALD and enhances mitochondrial generation, consequently alleviating mitochondrial damage caused by alcohol.

Consistent with the results of this study, COS increased the SIRT1 expression in an exercising rat model, promoted mitochondrial synthesis, and reduced blood lipid levels [37].

Long-term alcohol intake disrupts fatty acid  $\beta$  oxidation in hepatic cells, leading to fat accumulation in the liver. ACOX, ACSL, CPT1A, and CPT2, vital proteins related to



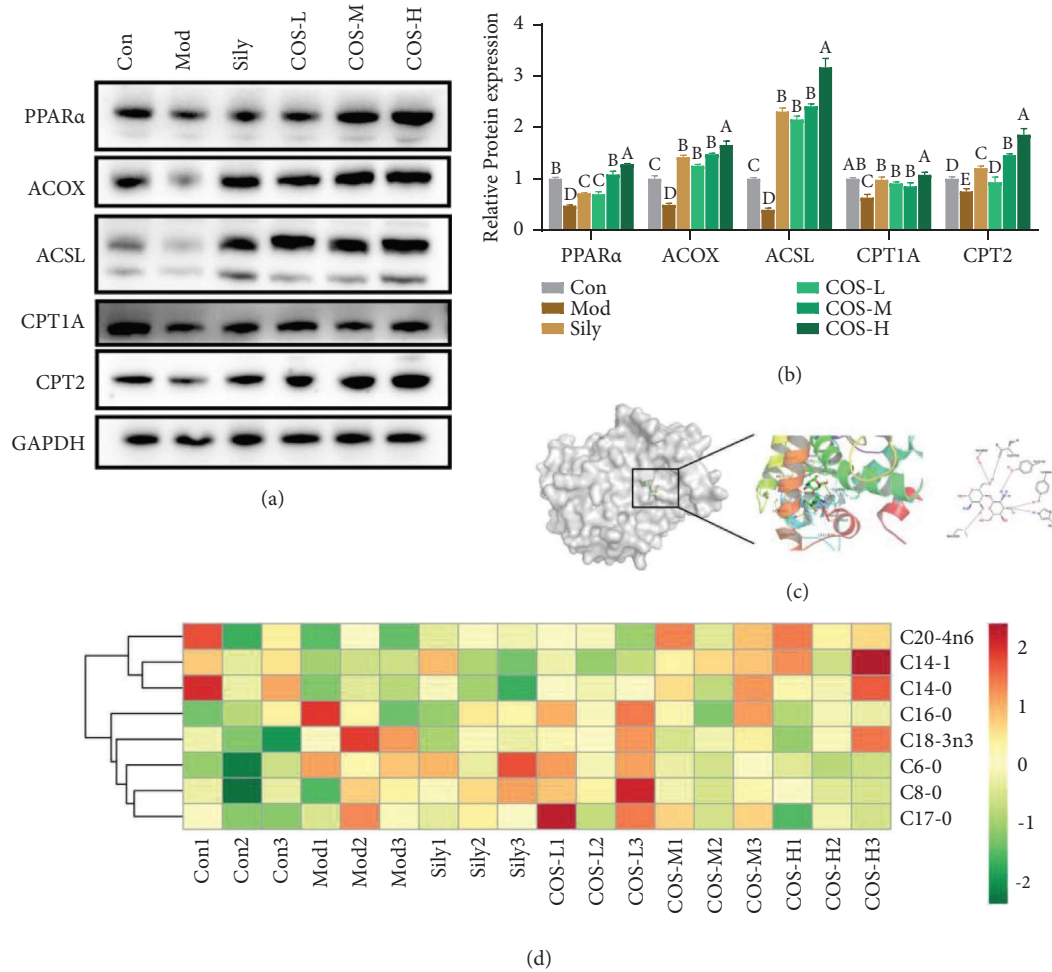


FIGURE 6: The effect of COS on hepatic fat metabolism in the chronic ALD mice. (a) The western blot image. (b) The relative PPAR $\alpha$ , ACOX, ACSL, CPT1A, and CPT2 protein expression is normalized to GAPDH. (c) The binding patterns, key interactions, and corresponding 2D maps of the active COS sites (green) relative to PPAR $\alpha$ , as revealed by molecular docking. (d) The representative fatty acid content in the liver. Data are shown as the mean  $\pm$  SD ( $n \geq 3$ ). Significant differences between the groups ( $P < 0.05$ ) are denoted by individual uppercase letters.

fatty acid  $\beta$  oxidation, are coregulated by PGC-1 and PPAR $\alpha$  [38, 39]. The results of this study indicated that PPAR $\alpha$ , ACOX, ACSL, CPT1A, and CPT2 were upregulated in response to COS in chronic ALD mice. COS promoted the CPT1A expression in an NAFLD model [40], activated PPAR $\alpha$  expression, and accelerated FFA catabolism [41]. Since PPAR $\alpha$  is an upstream factor that regulates  $\beta$  fatty acid oxidation, it is considered a potential target for COS to act in chronic ALD. Docking COS with PPAR $\alpha$  showed that COS generated effective hydrogen bonds at the active PPAR $\alpha$  site, acting similarly to a PPAR $\alpha$  agonist.

Since lipid metabolism is closely related to fatty acid  $\beta$  oxidation, this study also examined the fatty acid changes in the liver, the levels of which were restored to normal levels after COS intervention. The levels of saturated fatty acids such as palmitic and heptadecanoic acid in the liver decreased due to the upregulation of fatty acid  $\beta$  oxidation. Consistent with a study by Johnson [42], this paper revealed changes in the unsaturated fatty acid levels during chronic ALD, particularly a significant increase in serum linoleic acid levels. Linoleic acid accumulation

increased the production of proinflammatory products and oxidized LA metabolites, elevating the inflammatory response in the liver and leading to further damage [43]. Conversely, COS protected the liver from the alcohol-induced inflammatory response by reducing the linoleic acid level.

Several studies have demonstrated that ethanol exposure compromises the integrity of the intestinal barrier and damages the intestinal mucosa [44]. Alcohol downregulated the intestinal TJ and AJ proteins, leading to intestinal leakage and allowing bacteria and their products to enter the enterohepatic circulation, further damaging the liver [13, 15]. However, both medium- and high-dose COS treatments significantly upregulated the AJ and TJ protein levels, effectively reshaped intestinal permeability, improved intestinal leakage, and alleviated ALD. Feng et al. reported that COS promoted the ZO-1, occludin, and claudin1 expression while reversing LPS-induced intestinal barrier damage [23]. In addition, the current study results demonstrated for the first time that COS helped restore AJ protein levels in the gut.

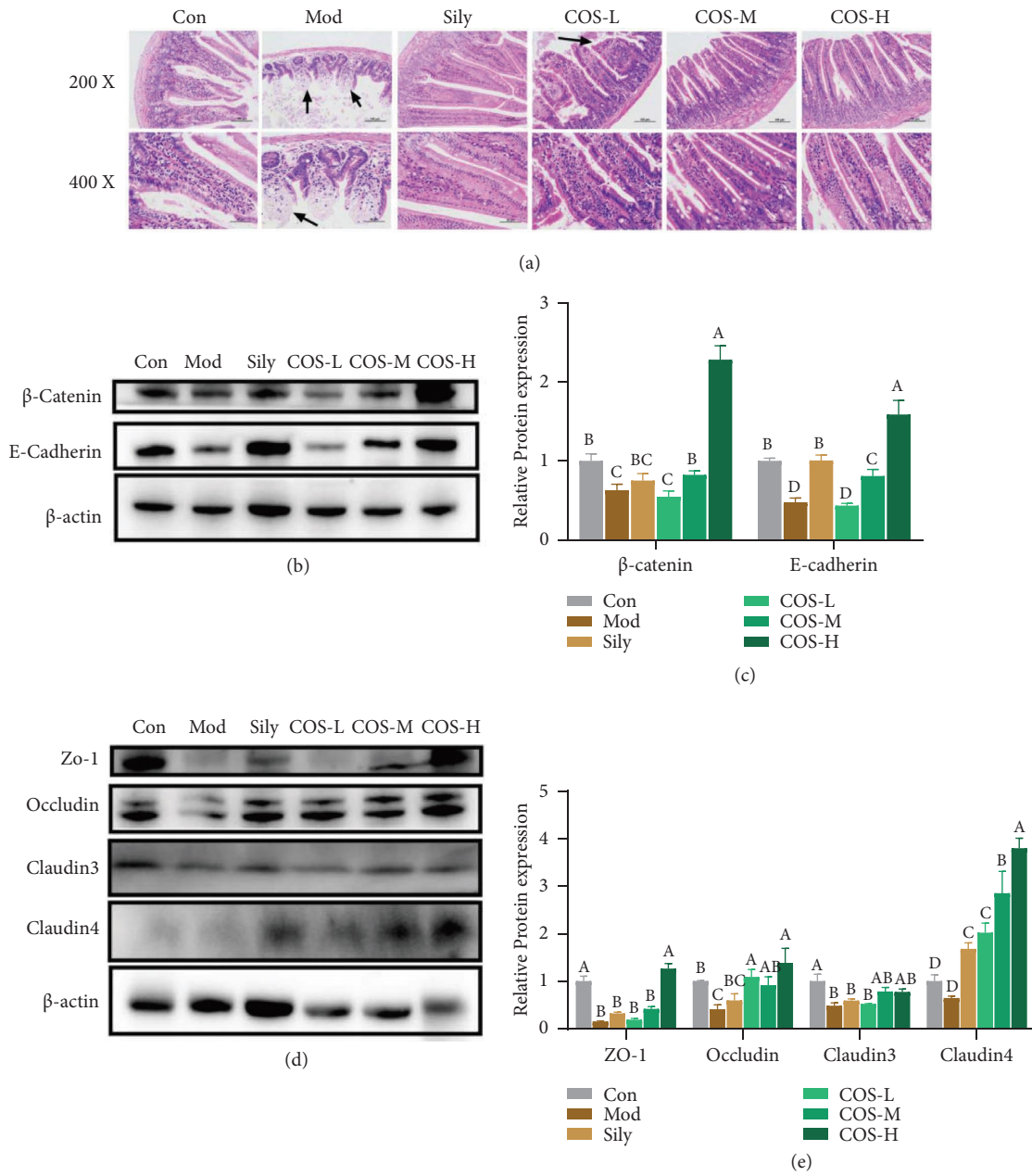


FIGURE 7: The effect of COS on the intestinal barrier of the mice with chronic ALD. (a) HE staining of the ileal tissue at 200 $\times$  (scale bar = 100  $\mu$ m) and 400x magnification (scale bar = 50  $\mu$ m). The black arrows indicate deformed small intestinal villi. (b) The western blot image of the AJ proteins. (c) The relative  $\beta$ -catenin and E-cadherin protein expression is normalized to  $\beta$ -actin. (d) The western blot image of the TJ proteins. (e) The relative ZO-1, occludin, claudin3, and claudin4 protein expression is normalized to  $\beta$ -actin. Data are shown as the mean  $\pm$  SD ( $n \geq 3$ ). Significant differences between the groups ( $P < 0.05$ ) are denoted by individual uppercase letters.

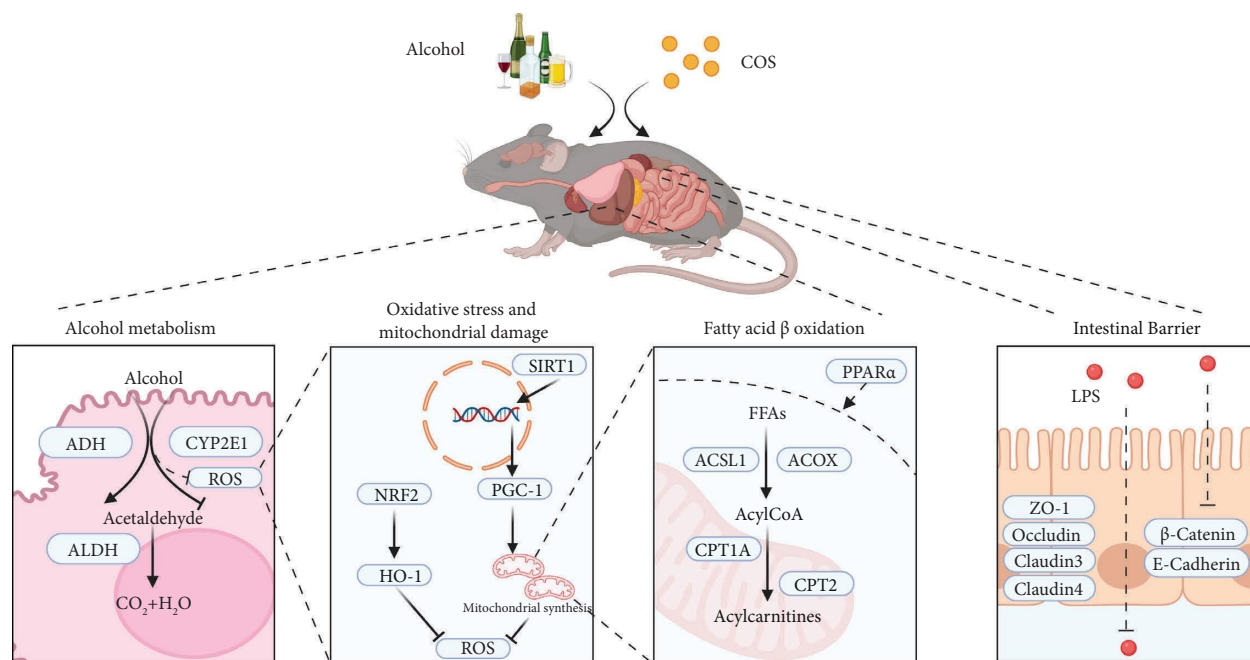


FIGURE 8: COS alleviates chronic ALD. The potential COS mechanism modifies chronic ALD by regulating alcohol metabolism, oxidative stress, fatty acid  $\beta$  oxidation, and the intestinal barrier.

## 5. Conclusion

This study demonstrates that COS can protect against chronic ALD in mice by improving alcohol metabolism, alleviating oxidative stress and mitochondrial damage, promoting fatty acid metabolism, and enhancing intestinal barrier function. The results provide a new perspective on the effects of COS intervention in chronic ALD. Moreover, it establishes a foundation for the further use of COS to regulate different metabolic lipid disorders.

## Data Availability

The data used to support the results of this study are available upon request from the corresponding author.

## Ethical Approval

Approval for the experiments was provided by the Ethics Committee of the East China University of Science and Technology (certificate no. ECUST-2022-082), which was conducted according to the China Institutional Animal Care and Use Committee requirements.

## Conflicts of Interest

The authors declare no conflicts of interest.

## Authors' Contributions

Yuan Li participated in the experiments, analyzed the data, designed the study, and wrote the manuscript. Jiaqi Zou provided raw materials and participated in the experiments. Hao Yin provided guidance, conducted methodological

research, and provided resources. Mengyao Zhao revised and edited the manuscript, provided guidance, conducted methodological research, and provided resources. Liming Zhao was responsible for revising the manuscript, supervision, and funding. All the authors discussed the results and approved the final manuscript.

## Acknowledgments

This work was supported by the Shanghai Frontiers Science Center of Optogenetic Techniques for Cell Metabolism (Shanghai Municipal Education Commission) and the Programme of Introducing Talents of Discipline to Universities (No. B18022).

## Supplementary Materials

The identification of COS was investigated by electrospray ionization source mass and high-performance liquid chromatography. Supplementary Figure 1. Electrospray ionization source mass spectra of COS. Supplementary Figure 2. High-performance liquid chromatography of COS. (*Supplementary Materials*)

## References

- [1] L. Ming, B. Qi, S. Hao, and R. Ji, "Camel milk ameliorates inflammatory mechanisms in an alcohol-induced liver injury mouse model," *Scientific Reports*, vol. 11, no. 1, Article ID 22811, 2021.
- [2] H. K. Seitz, R. Bataller, H. C. Pinto et al., "Publisher correction: alcoholic liver disease," *Nature Reviews Disease Primers*, vol. 4, 2018.
- [3] S. K. Ramaiah, C. Rivera, and G. E. Arteel, "Early-phase alcoholic liver disease: an update on animal models, pathology,

- and pathogenesis,” *International Journal of Toxicology*, vol. 23, no. 4, pp. 217–231, 2004.
- [4] M. Wang, X. Zhang, K. Feng et al., “Dietary  $\alpha$ -linolenic acid-rich flaxseed oil prevents against alcoholic hepatic steatosis via ameliorating lipid homeostasis at adipose tissue-liver axis in mice,” *Scientific Reports*, vol. 6, no. 1, Article ID 26826, 2016.
  - [5] S. Wang, T. Wan, M. Ye et al., “Nicotinamide riboside attenuates alcohol induced liver injuries via activation of Sirt1/PGC-1 $\alpha$ /mitochondrial biosynthesis pathway,” *Redox Biology*, vol. 17, pp. 89–98, 2018.
  - [6] A. Namachivayam and A. Valsala Gopalakrishnan, “A review on molecular mechanism of alcoholic liver disease,” *Life Sciences*, vol. 274, Article ID 119328, 2021.
  - [7] S. Jeon and R. Carr, “Alcohol effects on hepatic lipid metabolism,” *Journal of Lipid Research*, vol. 61, no. 4, pp. 470–479, 2020.
  - [8] R. Feng, L. Ma, M. Wang et al., “Oxidation of fish oil exacerbates alcoholic liver disease by enhancing intestinal dysbiosis in mice,” *Communications Biology*, vol. 3, no. 1, Article ID 481, 2022.
  - [9] H. K. Seitz and M. G. Neuman, “The history of alcoholic liver disease: from an unrecognized disease to one of the most frequent diseases in hepatology,” *Journal of Clinical Medicine*, vol. 10, no. 4, p. 858, 2021.
  - [10] N. Aosna, K. Rasineni, M. Ganesan, T. M. Donohue, and K. K. Kharbanda, “Pathogenesis of alcohol-associated liver disease,” *Journal of Clinical and Experimental Hepatology*, vol. 12, 2022.
  - [11] Q. Fang, X. Qiao, X. Q. Yin et al., “Flavonoids from *Scutellaria amoena* C. H. Wright alleviate mitochondrial dysfunction and regulate oxidative stress via Keap1/Nrf2/HO-1 axis in rats with high-fat diet-induced nonalcoholic steatohepatitis,” *Biomedicine and Pharmacotherapy*, vol. 158, Article ID 114160, 2023.
  - [12] R. Rao, “Endotoxemia and gut barrier dysfunction in alcoholic liver disease,” *Hepatology*, vol. 50, no. 2, pp. 638–644, 2009.
  - [13] Y. Cho, L. Yu, M. A. Abdelmegeed, S. Yoo, and B. J. Song, “Apoptosis of enterocytes and nitration of junctional complex proteins promote alcohol-induced gut leakiness and liver injury,” *Journal of Hepatology*, vol. 69, 2018.
  - [14] P. K. Shukla, A. S. Meena, K. Dalal et al., “Chronic stress and corticosterone exacerbate alcohol-induced tissue injury in the gut-liver-brain axis,” *Scientific Reports*, vol. 11, no. 1, Article ID 826, 2021.
  - [15] W. Rungratanawanich, Y. Lin, X. Wang, T. Kawamoto, S. B. Chidambaram, and B. J. Song, “ALDH2 deficiency increases susceptibility to binge alcohol-induced gut leakiness, endotoxemia, and acute liver injury in mice through the gut-liver axis,” *Redox Biology*, vol. 59, Article ID 102577, 2023.
  - [16] A. K. Singal, R. Bataller, J. Ahn, P. S. Kamath, and V. H. Shah, “ACG clinical guideline: alcoholic liver disease,” *American Journal of Gastroenterology*, vol. 113, no. 2, pp. 175–194, 2018.
  - [17] V. Subramaniam, S. Chakravarthi, R. Jegasothy et al., “Alcohol-associated liver disease: a review on its pathophysiology, diagnosis and drug therapy,” *Toxicology Reports*, vol. 8, pp. 376–385, 2021.
  - [18] S. Liu, R. Chen, and M. Chiang, “Effects of chitosan oligosaccharide on plasma and hepatic lipid metabolism and liver histomorphology in normal sprague-dawley Rats,” *Marine Drugs*, vol. 18, no. 8, p. 408, 2020.
  - [19] A. Chen, T. Taguchi, K. Sakai, Y. Matahira, M. Wang, and I. Miwa, “Effect of chitobiose and chitotriose on carbon tetrachloride-induced acute hepatotoxicity in rats,” *Biological and Pharmaceutical Bulletin*, vol. 28, no. 10, pp. 1971–1973, 2005.
  - [20] J. Xiang, J. Wang, H. Xie et al., “Protective effect and mechanism of chitooligosaccharides on acetaminophen-induced liver injury,” *Food and Function*, vol. 12, no. 20, pp. 9979–9993, 2021.
  - [21] P. Liu, H. Li, R. Li et al., “Nanoencapsulation of chitooligosaccharides enhances its oral bioavailability and anti-liver fibrotic effects,” *Food Research International*, vol. 157, Article ID 111471, 2022.
  - [22] X. Shen, X. Liang, X. Ji et al., “CD36 and DGAT2 facilitate the lipid-lowering effect of chitooligosaccharides via fatty acid intake and triglyceride synthesis signaling,” *Food and Function*, vol. 12, no. 18, pp. 8681–8693, 2021.
  - [23] J. Feng, Y. Liu, J. Chen et al., “Marine chitooligosaccharide alters intestinal flora structure and regulates hepatic inflammatory response to influence nonalcoholic fatty liver disease,” *Marine Drugs*, vol. 20, no. 6, p. 383, 2022.
  - [24] Z. Luo, X. Dong, Q. Ke, Q. Duan, and L. Shen, “Chitooligosaccharides inhibit ethanol-induced oxidative stress via activation of Nrf2 and reduction of MAPK phosphorylation,” *Oncology Reports*, vol. 32, no. 5, pp. 2215–2222, 2014.
  - [25] J. Park, K. S. Kwon, W. K. Jung, and Y. K. Lee, “Effects of chitooligosaccharide on alcohol dehydrogenase and aldehyde dehydrogenase in sprague-dawley rat after acute ethanol administration,” *Journal of Chitin and Chitosan*, vol. 11, 2006.
  - [26] X. Ji, L. Zhu, K. Chang et al., “Chitooligosaccharides: digestion characterization and effect of the degree of polymerization on gut microorganisms to manage the metabolome functional diversity in vitro,” *Carbohydrate Polymers*, vol. 275, Article ID 118716, 2022.
  - [27] A. Bertola, S. Mathews, S. H. Ki, H. Wang, and B. Gao, “Mouse model of chronic and binge ethanol feeding (the NIAAA model),” *Nature Protocols*, vol. 8, no. 3, pp. 627–637, 2013.
  - [28] M. P. Salaspuro, S. Shaw, E. Jayatilleke, W. A. Ross, and C. S. Lieber, “Attenuation of the ethanol-induced hepatic redox change after chronic alcohol consumption in baboons: metabolic consequences in vivo and in vitro,” *Hepatology*, vol. 1, no. 1, pp. 33–38, 1981.
  - [29] L. E. Martikainen, M. Rahnasto-Rilla, S. Neshybova, M. Lahtela-Kakkonen, H. Raunio, and R. O. Juvonen, “Interactions of inhibitor molecules with the human CYP2E1 enzyme active site,” *European Journal of Pharmaceutical Sciences*, vol. 47, no. 5, pp. 996–1005, 2012.
  - [30] Y. Liu, X. Feng, W. Jia, Z. Jing, W. Xu, and X. Cheng, “Virtual identification of novel PPAR $\alpha$ / $\gamma$  dual agonists by 3D-QSAR, molecule docking and molecular dynamics studies,” *Journal of Biomolecular Structure and Dynamics*, vol. 38, no. 9, pp. 2672–2685, 2020.
  - [31] W. Zhao, D. Peng, W. Li et al., “Probiotic-fermented *Pueraria lobata* (Willd.) Ohwi alleviates alcoholic liver injury by enhancing antioxidant defense and modulating gut microbiota,” *Journal of the Science of Food and Agriculture*, vol. 102, no. 15, pp. 6877–6888, 2022.
  - [32] L. Zhu, J. Xu, H. Li et al., “Berberine ameliorates abnormal lipid metabolism via the adenosine monophosphate-activated protein kinase/sirtuin 1 pathway in alcohol-related liver disease,” *Laboratory Investigation*, vol. 103, no. 4, Article ID 100041, 2023.
  - [33] R. Hou, X. Liu, X. Wu, M. Zheng, and J. Fu, “Therapeutic effect of natural melanin from edible fungus *Auricularia auricula* on alcohol-induced liver damage in vitro and in vivo,” *Food Science and Human Wellness*, vol. 10, no. 4, pp. 514–522, 2021.

- [34] Q. Mei, J. Hu, Z. Huang et al., "Pretreatment with chitosan oligosaccharides attenuate experimental severe acute pancreatitis via inhibiting oxidative stress and modulating intestinal homeostasis," *Acta Pharmacologica Sinica*, vol. 42, no. 6, pp. 942–953, 2021.
- [35] Y. Hussain, J. Singh, W. Raza et al., "Purpurin ameliorates alcohol-induced hepatotoxicity by reducing ROS generation and promoting Nrf2 expression," *Life Sciences*, vol. 309, Article ID 120964, 2022.
- [36] J. Silva, M. H. Spatz, C. Folk et al., "Dihydromyricetin improves mitochondrial outcomes in the liver of alcohol-fed mice via the AMPK/Sirt-1/PGC-1 $\alpha$  signaling axis," *Alcohol*, vol. 91, pp. 1–9, 2021.
- [37] H. W. Jeong, S. Y. Cho, S. Kim et al., "Chitoooligosaccharide induces mitochondrial biogenesis and increases exercise endurance through the activation of Sirt1 and AMPK in rats," *PLoS One*, vol. 7, no. 7, Article ID e40073, 2012.
- [38] J. K. Reddy and T. Hashimoto, "Peroxisomal beta-oxidation and peroxisome proliferator-activated receptor alpha: an adaptive metabolic system," *Annual Review of Nutrition*, vol. 21, 2001.
- [39] M. You, A. Jogasuria, C. Taylor, and J. Wu, "Sirtuin 1 signaling and alcoholic fatty liver disease," *Hepatobiliary Surgery and Nutrition*, vol. 4, no. 2, pp. 88–100, 2015.
- [40] J. Wang, M. Jiang, Y. Xin, N. Geng, X. Li, and S. Xuan, "Effect of chitoooligosaccharide on hepatic triglyceride metabolism and related mechanisms," *Chinese Journal of Hepatology*, vol. 24, 2016.
- [41] Y. Jiang, C. Fu, G. Liu, J. Guo, and Z. Su, "Cholesterol-lowering effects and potential mechanisms of chitoooligosaccharide capsules in hyperlipidemic rats," *Food and Nutrition Research*, vol. 62, no. 0, 2018.
- [42] S. B. Johnson, E. G. Gordon, C. McClain, G. Low, and R. T. Holman, "Abnormal polyunsaturated fatty acid patterns of serum lipids in alcoholism and cirrhosis: arachidonic acid deficiency in cirrhosis," *Proceedings of the National Academy of Sciences*, vol. 82, no. 6, pp. 1815–1818, 1985.
- [43] D. Lin, X. Jiang, Y. Zhao, X. Zhai, and X. Yang, "Komagataeibacter hansenii CGMCC 3917 alleviates alcohol-induced liver injury by regulating fatty acid metabolism and intestinal microbiota diversity in mice," *Food and Function*, vol. 11, no. 5, pp. 4591–4604, 2020.
- [44] S. Liu, H. Liu, S. Wang, C. Zhang, F. Guo, and T. Zeng, "Diallyl disulfide ameliorates ethanol-induced liver steatosis and inflammation by maintaining the fatty acid catabolism and regulating the gut-liver axis," *Food and Chemical Toxicology*, vol. 164, Article ID 113108, 2022.